



HAL
open science

In-Mold Electronics on Poly(Lactic Acid): towards a more sustainable mass production of plastronic devices

Caroline Goument, Tony Gerges, Philippe Lombard, Hayet Lakhdar, Murat Arli, Valernst Martial Gilmus, Simon A. Lambert, Bruno Allard, J-y Charneau, Michel Cabrera

► To cite this version:

Caroline Goument, Tony Gerges, Philippe Lombard, Hayet Lakhdar, Murat Arli, et al.. In-Mold Electronics on Poly(Lactic Acid): towards a more sustainable mass production of plastronic devices. International Journal of Advanced Manufacturing Technology, 2023, 125 (5-6), pp.2643-2660. 10.1007/s00170-023-10878-4 . hal-04069897

HAL Id: hal-04069897

<https://hal.science/hal-04069897>

Submitted on 16 May 2023

HAL is a multi-disciplinary open access archive for the deposit and dissemination of scientific research documents, whether they are published or not. The documents may come from teaching and research institutions in France or abroad, or from public or private research centers.

L'archive ouverte pluridisciplinaire **HAL**, est destinée au dépôt et à la diffusion de documents scientifiques de niveau recherche, publiés ou non, émanant des établissements d'enseignement et de recherche français ou étrangers, des laboratoires publics ou privés.

In Mold Electronics on Poly(lactic acid) – towards a more sustainable mass production of plastronic devices

Caroline GOUMENT^{1*}, Tony GERGES¹, Philippe LOMBARD¹, Hayet LAKHDAR², Murat ARLI², Valernst Martial GILMUS¹, Simon Auguste LAMBERT¹, Bruno ALLARD¹, Jean-Yves CHARMEAU^{2*}, Michel CABRERA^{1*}

¹ Univ Lyon, INSA Lyon, Université Claude Bernard Lyon 1, Ecole Centrale de Lyon, CNRS, Ampère, UMR 5005, 69621 Villeurbanne, France

² Univ Lyon, INSA Lyon, IMP, UMR 5223, 01100 Bellignat, France

Abstract

3D Plastronics is a technology capable of improving the integration of heterogeneous functions in or on polymer packages of electronic devices by implementation of conductive patterns and electronic components. Among 3D Plastronics technologies, In Mold Electronics (IME) is a fast-growing emerging manufacturing process for mass production of plastronic devices. It is based on the screen printing of a thermoplastic film (printed electronic process), followed by a 3D shaping using thermoforming and finally a step of over-molding by injection of a thermoplastic polymer. Nowadays, IME is mainly based on PolyCarbonate (PC), which is thus a reference material. The paper focuses on Poly(Lactic Acid) (PLA), a biosourced and biodegradable polymer to reduce the environmental impact of IME manufacturing. The thermal and mechanical properties of the PLA materials are investigated to optimize the IME process parameters and to take into account the glass transition temperature T_g around 55-60°C of PLA. Thermal properties of inks are then considered to adapt drying to the polymer substrate, with the results being a good adhesion (category 0 of the ISO 2409 standard) and sufficient electrical resistivity (290 $\mu\Omega\cdot\text{cm}$) of the ink on PLA. Electronic components are connected to the circuit with conductive and structural pastes giving a shear stress of 9.1 N/mm² on PLA. The next steps of the IME process are also studied, thermoforming and injection molding. An electronic circuit is designed as a demonstration vehicle combining the IME process with PLA as main structural material.

Keywords 3D Plastronics, Poly(Lactic Acid), In Mold Electronics, PolyCarbonate, mass production

1. Introduction

3D Plastronics is a technology capable of improving the integration of heterogeneous functions in or on polymer packages of electronic systems, functions which are no longer limited to mechanical aspects. The main principle is to implement conductive patterns and electronic components, such as Surface Mount Devices (SMDs), on the 3D surface of a device package in order to simplify connections, better organize components and generally improve the interaction of electronic, mechatronic, optical and/or thermal functions.

To manufacture plastronic devices, Laser Direct Structuring (LDS) [1] and two-shot injection molding [2] are used for mass production, whereas other technologies such as Laser Subtractive Structuring [3], aerosol jet [4] and direct ink writing [5], among others, are also available but for a smaller production scale. Such manufactured devices are sometimes named “3D-Molded Interconnect Devices” (3D-MID), although (according to us) 3D-MID should only refer to the LDS process (see [6] for a review on LDS and the other manufacturing processes).

In addition to the latter technologies, In Mold Electronics (IME), also called In Mold Structural Electronics (IMSE) [7] is emerging as a new manufacturing process for mass production of plastronic devices [8, 9].

The principle of IME is illustrated in Fig.1 and involves three main steps. The first step (Fig.1a) consists in printing the conductive patterns with a conductive ink on a thin thermoplastic film (thickness of 300-400 μm), which constitutes the substrate of the plastronic device. Other inks such as decorative or insulating inks can also be deposited as needed but are not discussed in this paper. After printing each layer, the ink is dried, typically in a heat chamber. Then electronic components, such as SMDs, are placed on the film and connected to the conductive pattern with an electrically conductive adhesive. If necessary non-conductive structural adhesives or

*Corresponding authors: caroline.goument@insa-lyon.fr (ORCID: <https://orcid.org/0000-0003-4866-7536>); michel.cabrera@insa-lyon.fr; jean-yves.charmeau@insa-lyon.fr

even glob top resins can also be deposited to better hold the SMDs in place. In the second step (Fig.1b), the film carrying the conductive network and the SMDs is shaped in three dimensions using a thermoforming tool by applying heat and pressure. At this stage, the deformability and adhesion of the inks onto the film are essential, as well as the adhesion of the SMDs. In the third step, the contour of the device is freed from the film by die-cutting or trimming and placed in the cavity of an injection mold. The non-printed surface of the polymer film is placed against the surface of the mold so that the conductive paths and SMDs are over-molded (Fig.1c).

The final plastronic part is an electronic device embedded in a 3D-shaped thermoplastic sheet whose thickness is about 3-4 mm. Thus, the electronic circuit (SMDs and conductive paths) is protected by the polymer layers from outside aggressions in the environment.

For mass production, IME has significant advantages over LDS and two-step injection molding. In the former case, the conductive pattern is printed directly on the film while in the latter case, it is produced by electroless deposition (ELD) after the injection step, which requires thermoplastic pellets charged with a catalyst. ELD uses polluting chemicals with specific chemical installations, which is a major drawback. Indeed, only well-known 2D machines in the field of Printed Electronics (PE) (screen printing, inkjet printing, dispensing, etc.), current polymer shaping technologies (thermoforming, injection molding) and conventional raw materials (pellets, films) are considered in IME. Moreover, in the IME process, conventional industrial machines can pick up and place the SMDs on the film substrate. In contrast, in the LDS or two-step injection molding processes, SMDs must be placed on complex 3D surfaces, which requires expensive and unconventional tools.

However, IME has also inherent drawbacks. The electrical resistivity of conductive inks, commonly based on silver flakes, is at best about $40 \mu\Omega\cdot\text{cm}$, which is much higher than the resistivity of electroless copper ($2.2 \mu\Omega\cdot\text{cm}$ [10]). Also, in terms of geometry freedom in 3D design, IME is more limited than the others.

In any case, IME is a promising technology for mass production, allowing completely new opportunities. For example, IME parts are often used as smart surfaces for new Human-Machine-Interface (HMI) with capacitive sensors and lightings [11]. These are embedded in the polymer object but there is a possibility of direct human interaction through the original thin polymer film. In the future, haptic systems may also be of interest [12].

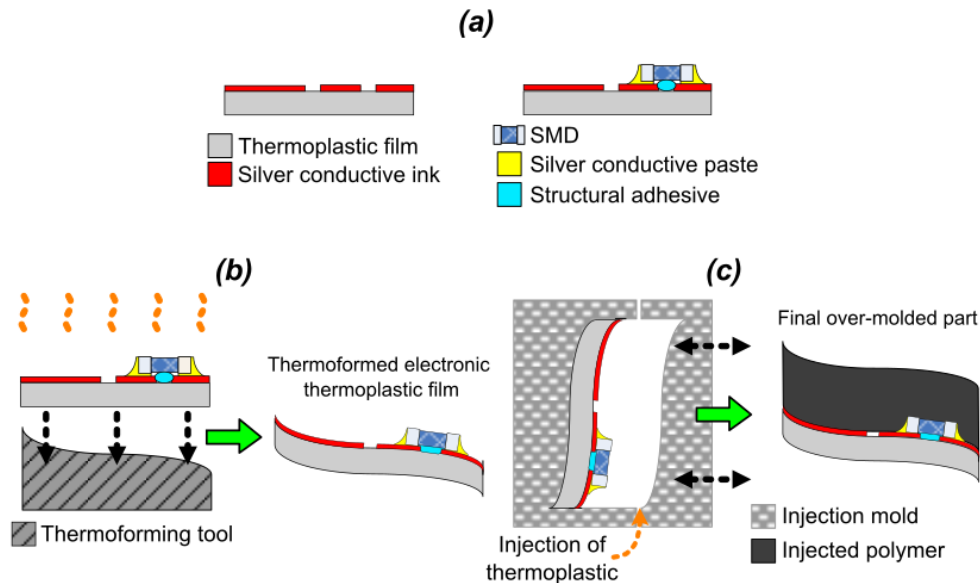


Fig. 1 IME manufacturing steps: (a) screen printing of conductive ink and adhesion of SMDs, (b) thermoforming, (c) over-molding by injection

Regarding the raw materials, PolyCarbonate (PC) is nowadays widely used in many industrial applications (automotive, construction, optical, etc). It is also the reference polymer material in IME [6, 9, 13-15]. The reason is that PC is an amorphous polymer easy to thermoform with excellent mechanical and thermal properties. Commercial stretchable inks have been designed to be used specifically with PC, thus offering a good adhesion coefficient [11, 16]. PC also withstands the thermal postprocessing such as heat curing at 120°C for 20 minutes as recommended by the supplier, to obtain good intrinsic properties for the inks (e.g. resistivity for conductive inks) and good adhesion to the film.

However, for the sake of sustainability, the perspective of mass production with IME underlines the necessity to replace PC with a more ecofriendly material. Therefore, the aim of this work is to assess whether Poly(Lactic Acid) (PLA) is a valid alternative to PC. PLA is one of few biosourced polymers and it is easy to implement by

extrusion or injection molding. The world production of bioplastics is estimated at nearly 2 Mt/year with the demand in PLA increasing rapidly in the last years (from 10% of the world bioplastics production in 2017 to 19.5% in 2020 [17, 18]) making it an interesting choice for mass production of IME devices. In addition, it can be recycled by mechanical means, mixed with new materials to be reused or even depolymerized, which can pave the way for a circular economy [19].

To the best of our knowledge, the use of PLA in the different steps of the IME process has not been investigated although this is critical for developing sustainable electronic systems. Therefore, this work aims to study the potential replacement of PC by PLA in the IME process. This article is organized as follows: after a review of the state of the art on PC and PLA materials, as well as on IME, each step of the manufacturing process is studied using PLA. Next, the manufacturing of a functional IME plastronic system in PLA is reported to demonstrate a proof of concept. Finally, a detailed discussion is carried out to analyze future directions for improvement before considering an industrial-scale change.

2. Polymers for IME

2.1. PolyCarbonate

PolyCarbonate (PC) is an amorphous thermoplastic polymer which was first discovered in the 1950s [20]. Today, it is obtained from the interfacial polycondensation occurring between bisphenol A and phosgene in the presence of sodium hydroxide. Fig. 2 shows the chemical structure of PC. It is important to note that the chemical compounds used in the synthesis of PC are dangerous for the human health: phosgene is an odorless and toxic gas at room temperature and bisphenol A is a carcinogenic petrochemical substance. However, PC is commonly recycled mechanically, reused and mixed with virgin materials to manufacture new objects. This is the most common method to recycle petroleum-based polymers but it is not an endless cycle mainly because the mechanical properties of PC are degraded. After 5 to 7 cycles, the polymer properties are too degraded for the material to be reused and it has to be destroyed.

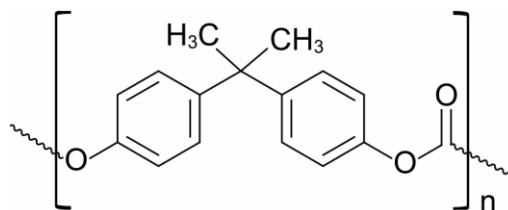


Fig. 2 Chemical formula and structure of PolyCarbonate

2.2. Poly(Lactic Acid)

Poly(Lactic acid) (PLA) is a thermoplastic polymer. It is one of the few biodegradable and bio-based materials derived from renewable resources (corn starch, sugar cane) [19]. Its chemical structure is shown in Fig. 3a. At industrial scale, the most common way to synthesize PLA is the ring opening polymerization of lactide in the presence of a catalyst. PLA is chemically reactive due to the presence of hydroxide groups -OH at both ends of the molecule backbone. This polymer is considered as one of the best substitutes for petroleum-based polymers and is used in many applications such as automotive, packaging and electronic industries [21-23]. The recent growing interest in PLA is motivated by the need for an environmentally friendly material that has good mechanical properties [24] such as a high elastic modulus. The alternative of PLA would enable a more sustainable mass production of IME parts in the long run. However, PLA has also several drawbacks as it is very brittle and its glass transition temperature (T_g) is close to 60°C only, which may be an issue for the curing conditions of the inks.

In other respects, the lactic acid is known to have two isomers L and D (presented in Fig. 3b), which means that various forms of PLA molecules are available [25]:

- Poly-L-lactide (PLLA), which contains at least 99.5% of L-isomers.
- Standard PLA has 85% to 99.5% of L- isomers completed by D-isomers.
- Poly-D-lactide (PDLA), which is composed of 100% of D-isomers.

There also exists a stereocomplex (or racemic lactide) with 50% PLLA and 50% PDLA. Therefore, each PLA grade has its own level of crystallinity.

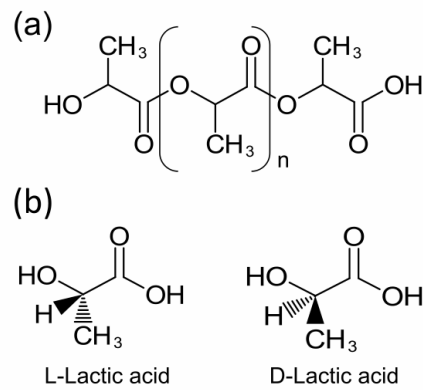


Fig. 3 (a) PLA molecular structure and (b) lactic acid stereoisomers

PLA can be either in an amorphous or semi-crystalline state, depending on its stereochemistry and thermal history. With more than 8% of D-isomers, PLA does not crystallize and is therefore amorphous. Between 0% and 8% of D-isomers, crystals appear in the PLA structure making it a semi-crystalline polymer. In addition, PLA is considered as a polymorphic polymer, which means that it contains several crystal forms depending on the crystallization conditions and therefore the thermal history of the material.

- The most crystalline form of PLA is PLLA and three different crystalline sub-structures α , β , and γ of PLLA have been identified. The α crystal form is the most common [26] and is identified as an helix with an orthorhombic unit cell [27]. In fact, this polymer exhibits low crystallization kinetics, making it an easy-to-prepare material with a broad range of degrees of crystallinity which explains its extensive use in 3D printing by Fused Deposition Modeling (FDM), and makes it a suitable candidate for the production of 3D polymer shapes by thermoforming or injection molding [28].

The factors mainly influencing the crystallization kinetics of PLA are its molecular mass, its D-isomers content, the type of crystal form, the amount of impurities, the thermal treatments undergone or even the manufacturing method. For instance, the higher the crystallinity, the denser the polymer, which in thermoforming and injection molding means more thermal shrinkage [29]. Therefore, a high level of crystallinity will have a negative impact on the shaping of the polymer during the IME process but it is desirable for better thermal and mechanical properties of PLA [30].

2.3. Comparison of properties

Properties of PLA and PC are listed in Table 1. The crystalline part of PLA has a melting temperature T_m ranging from 130°C (PLA with 2% to 5% D-isomers) to 175°C (PLLA). In comparison, PC is a material favored for technical applications because of its excellent transparency, high T_g (around 150°C) and great impact resistance [31]. The Izod impact strength test is a standardized method to determine the impact resistance of materials using the potential energy of a pendulum.

Table 1 Main thermal and mechanical properties of PLA compared to PC [27, 32, 33].

	PLA	PC
<i>Thermal properties</i>		
T _g (°C)	55 – 65	150
T _m (°C)	130 – 175	/
T _d (°C)	240	370
Thermal conductivity (W/m.K)	0.13 – 0.16	0.19 – 0.21
CTE (1/°C)	126 – 145.10 ⁻⁶	70.10 ⁻⁶
<i>Mechanical properties</i>		
Density	1.24	1.2
Tensile strength (MPa)	60	65
Elongation at break (%)	5 – 10	100
Elastic modulus (MPa)	3200 – 3500	2350
Izod (kJ/m ²)	2-4 (notched)	12 (notched)

2.4. The In Mold Electronics technology

Fig.1a, *screen printing* consists in transferring a pattern on a flat surface using a mesh screen, ink and a squeegee. Basically, with a stencil on a fine mesh screen, the ink is pushed through with the pressure of the squeegee to create an imprint of the design on the surface beneath. An ink for Printed Electronics is composed of three basic elements [34, 35]: the solvent, the polymer resin and the filler. In the case of conductive inks, the filler is in general made of conductive microparticles (silver, copper, etc.) when using screen printing or nanoparticles when using ink jet printing (which is out of the scope of this article). Contrary to conventional inks for Printed Electronics, IME inks must withstand the deformation of the substrate during thermoforming and have to be stretchable. They must also withstand the stringent conditions of over-molding. Therefore, inks are specifically formulated to be deformed on a polymer substrate in IME [16]. With the screen-printing method, the thickness of the conductive paths is around 5-8 μm and their width depends on the design and mesh of the screen, the rheology of the ink and the surface properties of the film. In addition, switching a PC substrate with a PLA substrate will present us with issues regarding the ink performances [36], the drying conditions being different depending on the thermal properties of the polymer substrate considered.

Fig.1b, *thermoforming*: the thin polymer layer is held above the mold by a frame and heated up by radiation to a temperature enabling its deformation, which happens thanks to a vacuum under the softened polymer sheet [37]. Thermoplastic amorphous polymers (PC, PS, PMMA, ...) are easily thermoformable, whereas semi-crystalline polymers such as PLA are thermoformable but have poorer final mechanical properties: the higher their crystallinity, the more brittle they become. We found a paper about the properties of PLA films during thermoforming in simulation [38] but no detailed experimental work.

Fig.1c, *injection molding*: the polymer material is injected under pressure into a closed mold that defines the shape of the object to be produced. Inside the mold, the polymer is cooled until it reverts to a solid, then the finished part is ejected. During injection molding, the gap between the various material properties can cause unwelcome thermal shrinkages and shear stress at the interface between the molded polymer and the subassembly with the electronic components and conductive paths. This induces mechanical distortions of the over-molded object which can lead to system failures (joint fatigue, SMD delamination, substrate distortion) [29]. One major problem during injection molding is to prevent the conductive network and SMDs from washing out just as the injected polymer covers the structure. Liu et al. have observed this wash-off of the ink on PET substrate [39]. This problem has not been fully solved with the classic IME method on PC yet and will also be a point of interest for PLA.

3. Materials and experimental procedure

3.1. PC and PLA polymers

One grade of PC is selected for thermoforming (PC1 in Table 2) and one for over-molding (PC2). PC1 films were purchased and used as is. PC2 pellets were dried at 90°C in a heat chamber for 12h before use. As PLA films of sufficient thickness (about 300-400 μm) are not commercially manufactured, we extruded the films. Therefore, we used two kinds of PLA pellets: one for extrusion (PLA1 in Table 2) and one for over-molding (PLA2). PLA1 and PLA2 pellets were dried at 70°C under vacuum for 12h before processing. PLA1 films were extruded using a SCAMEX single-screw extruder, a profile temperature of 160-190-200-210°C from zone 1 to cast film die, a screw speed of 56 rpm and a chill roll temperature of 55°C. The obtained films feature a thickness of 300 μm . To reduce the internal stress created during extrusion, the films were compressed between two heavy metal plates and annealed at 75°C for 15 min at atmospheric pressure.

Table 2 Suppliers data for the polymers

	Supplier	Type	Grade	Data	Melt Flow Rate
PC1	Covestro	Film	Makrofol DE 1-1	Transparent	/
PC2	Covestro	Pellets for injection	2405	Transparent	19 cm ³ /10 min
PLA1	NatureWorks LLC	Pellets for extrusion	2003D	4.1% D-isomers	6.0 g/10 min
PLA2	NatureWorks LLC	Pellets for injection	3251D	1.6% D-isomers	80 g/10min

3.2. Conductive ink for screen printing

The conductive tracks were patterned by screen printing conductive ink with silver flakes ME603 (DuPont, USA) on PC1 and PLA1 films using a manual screen printer. The screens are made of a polyester mesh of 110 threads/cm with wires of 45 μm in diameter. The distance between the mesh and the substrate was set at 2 ± 0.5

mm. A constant pressure and speed were applied to the squeegee against the screen and substrate with an angle of 45°. All samples were produced with two successive passes, the first one to fill the screen with the ink and the second to print the pattern. Parameters were manually optimized and the reproducibility of the print was checked with five samples. To achieve optimum performances of the ink after printing, the screen-printed substrates were dried in a heat chamber at 120°C for 20 min for PC1 films and at 55°C for 2h30 for PLA1 films (as discussed in section 5.2).

3.3. Component assembly

Silver-filled conductive adhesive ME902 (DuPont, USA) was used to ensure electric conductivity between SMDs and ME603 ink (listed in Table 3). When necessary, ethyl cyanoacrylate (Loctite Superglue-3 from Henkel) was applied as structural non-conductive adhesive to improve the adhesion between SMDs and the film substrate. The two adhesives were dispensed using a dispensing machine CMS 450.V2 DOTTY (CIF, France) with a Luer-Lock syringe (20-gauge). Component placement was manually performed using anti-static tweezers. Adhesive drying was done in a heat chamber at 120°C for 20 min for PC1 films and at 55°C for 2h30 for PLA1 films (as discussed in section 5.2). The resulting “substrate” will be referred in the following sections as the electronic film.

Table 3 Supplier's data for the conductive ink and paste [40]

Conductive	Function	Resistivity	Shear strength
ME603 ink	Screen printing	89 $\mu\Omega$.cm	/
ME902 adhesive	SMD adhesion	250-350 $\mu\Omega$.cm	1-1.2 kgf

3.4. Thermoforming

The electronic film was fixed to a 270 x 240 mm frame of a Vacuum Former 1820 (CR Clarke, UK). The temperature was set at 190°C for PC and 110°C for PLA. The electronic film was vacuum formed over a 3D mold at -1 bar. A conical mold and circular molds with various dimensions (see Supplementary Information SI1) were 3D printed, using High Temperature resin (FLHTAM02), with a stereolithography printer (Form 3 - Formlabs, USA).

3.5. Injection molding

The PC1 electronic film was placed into a 150 x 100 x 2 mm rectangular plate mold mounted on a 200 HERCULE injection molding machine (Billion, France) and over-molded by injection of PC2 pellets. This mold is referred as “Injection Mold 1” in the following sections. The screw barrel was regulated at 310°C and holding pressure was 1600 bar for 10s. The injection mold temperature was set at 110°C.

The PLA1 electronic film was trimmed and placed into a 100 mm x 80 x 2.5 mm rectangular plate mold mounted on a BOY35E injection molding machine (Dr. Boy GmbH, Germany). This mold is referred as “Injection Mold 2” in the following sections. The PLA electronic film was over-molded by injection of PLA2 pellets. The screw barrel was regulated at 210°C and the injection pressure was 130 bar. The injection mold is at room temperature.

4. Characterization methods

Differential Scanning Calorimetry (DSC) and ThermoGravimetric Analysis (TGA) measurements were performed on PC and PLA with DSC Q20 and TGA Q50 (TA Instruments). The DSC cell was continuously purged with nitrogen at a flow rate of 50 mL/min. The samples (about 10-15 mg) were studied in non-isothermal mode with a first cycle (heat/cool) with a temperature ramp at 10°C/min and a second cycle at 5°C/min from 40°C to 230°C back to 40°C for PC and from 30°C to 200°C back to 30°C for PLA. All TGA measurements were carried out under nitrogen flow at 90 mL/min. The samples were subjected to a temperature ramp at 10°C/min from room temperature to 700°C (PC and conductive ink and adhesive) and to 600°C (PLA). Concerning the ME603 ink, the samples were also studied in isothermal mode at 55°C for 36h, and at 120°C for 1h.

Following the ISO 527-3 standard, the tensile tests were performed using the SHIMADZU Autograph AGS-X equipment on type 2 specimens chopped into the polymer films. The specimens were about 150 mm long and 20 mm wide. The analyses were performed at a rate of 50 mm/min, with a 1 N preload to obtain the tensile strength and the elongation at break. For Young’s modulus, the extensometer SHIMADZU ESA – CU200 was added to the setup and the experiments were done on the same type of specimens at a rate of 1 mm/min. The impact

resistance of the polymers was determined using an impact pendulum testing machine (Instron CEAST 9050, Illinois Tool Work Inc.). Specimens were prepared according to the ISO 179-1 standard, so rectangular samples of dimensions 80 x 10 x 4 mm. A 15J pendulum was used for PC specimens with a 2-mm notch whereas a 1J pendulum was used for unnotched and 2-mm notched PLA specimens.

The surface roughness S_a , expressed in μm , was determined to see the influence of the polymer film roughness on the surface energy. We used a numerical microscope (Hirox RH-2000, Japan) with a Nano Point Scanner (NPS-NP3, confocal profilometer). Contact angle measurements were also performed using two liquids, deionized water and diiodomethane, to determine the contact angles and the surface energy of the polymers. The Mobile Surface Analyser (MSA) from Krüss was used and the sessile drop method was applied. Eight measurements were performed for each sample.

The resistance R of 25 x 1 mm lines of conductive ink was measured using four-point aligned Tungsten Carbide probes with a radius of 125 μm and a width l of 1.27 mm connected to a Keithley 2450 SourceMeter. The cross-sectional area A of the ink track pattern was measured with a confocal profilometer NPS-NP3 mounted on a Hirox RH-2000 microscope. The resistivity ρ in $\mu\Omega\cdot\text{cm}$ was calculated as:

$$\rho = \frac{R \times A}{l} \quad (1)$$

A standardized cross-cut test following the ISO 2409 norm was carried out on a 50 x 50 mm screen printed surface to evaluate the adhesion of the conductive ink. Using a specific sharp tool and 2525 Scotch adhesive tape, lines were engraved in the ink to do a grid pattern and the screen-printed ink was peeled off rapidly and vertically using the tape at a 45° angle with the grid. The percentage area removed or deformed was used to reflect the adhesion and gave the corresponding adhesion quality (from 0 to 5) according to the classification in the standard.

The shear strength of the SMDs after connecting to the conductive ink and bonding was evaluated by a bond tester (XYZTEC Condor Sigma) under the following conditions: shear speed of 100 $\mu\text{m/s}$, shear height of 100 μm , and shear width of 1 mm. The fracture surfaces were examined and used to measure the surface area of the adhesive with the numerical microscopy Hirox RH-2000. The shear stress was then calculated by dividing the shear force by the measured surface area of the adhesive. The measures were performed on 10 resistors for each combination of adhesives.

5. Experimental results and discussion

5.1. Characterization of the polymer films

DSC analyses presented in Fig. 4 were carried out to examine the effect of the thermal properties of both polymers on the IME process. PC is an amorphous polymer; thus as expected, one glass transition was found whose experimental value of T_g (145°C) corresponds to the literature [41]. Regarding PLA1 and PLA2, the profile of the thermal properties also corresponds to the literature [21, 27]. The second heating at 5°C/min shows significant glass transition and melting temperatures. Thus, all the PLAs tested are semi-crystalline, which confirm the datasheet of the supplier (see Table 2 for D-isomers percentage). Surprisingly, the recrystallization during the cooling process is not noticeable on the DSC curves, but a small exothermic variation is visible in the heating process near 115°C before melting. Zhang et al. [42] considered that an α' (or newly named δ) crystalline form of PLA exists and grows under normal crystallization conditions. α' is a disorganized form of α . The transformation of the α' crystal into an α crystal occurs between 100 and 120°C, which corresponds to the exothermic variation observed on the DSC curves. Moreover, this cold crystallization shows that the crystallization kinetics of PLA is extremely slow and that PLA does not have time to crystallize at a cooling rate of 5°C/min.

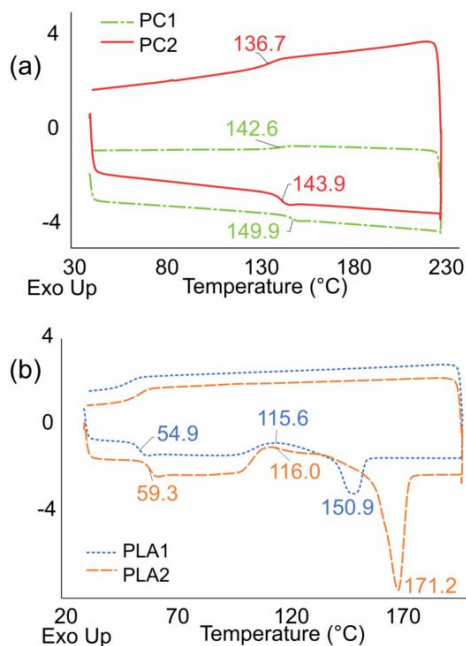


Fig. 4 DSC curves for the second cycle at 5°C/min of (a) PC and (b) PLA

Another remarkable aspect is the difference in melting temperature of the injection grade (171°C) which is greater than that of the extrusion grade (151°C). This corresponds to the difference of crystallinity that we evaluated with the DSC curve of the second cycle at 5°C/min and the following equation [43, 44]:

$$\chi_c = \frac{\Delta H_m - \Delta H_c}{\Delta H_m^\infty} \times 100 \quad (2)$$

With ΔH_m and ΔH_c the enthalpy variations of melting and crystallization respectively, and ΔH_m^∞ the melting enthalpy of 100% crystalline PLA (constant of 93.1 J/g).

The thermodynamic variables (enthalpies) to determine the crystallinity of PLA are indicated below in Table 4. Therefore, considering the slow crystallization kinetics and the low degree of crystallinity of both PLA (less than 5%), an important conclusion is that the PLA materials used in this work will have a more amorphous behavior than crystalline during thermoforming and injection molding. This explains the ease of thermoforming. Another consequence for possible lighting applications is that the final PLA device will have acceptable optical properties, although it is still less transparent than Polycarbonate.

Table 4 Thermodynamic variables of PLA materials obtained from the second heating cycle of DSC curves

Samples	ΔH_c (J/g)	ΔH_m (J/g)	χ_c (%)
PLA1	12.90	15.09	2.35
PLA2	30.43	35.00	4.91

In other respects, the degradation temperature and the final residue of all tested polymers can be observed by TGA analysis. Fig. 5 presents the results in non-isothermal mode. Both PC have a higher thermal resistance than both PLA. PC begins degrading at 454°C but slowly because the residue is more than 20% at 700°C. PLAs start degrading at a lower temperature of about 310°C but it goes quickly since the degradation is almost complete at 375°C with a residue of less than 1%.

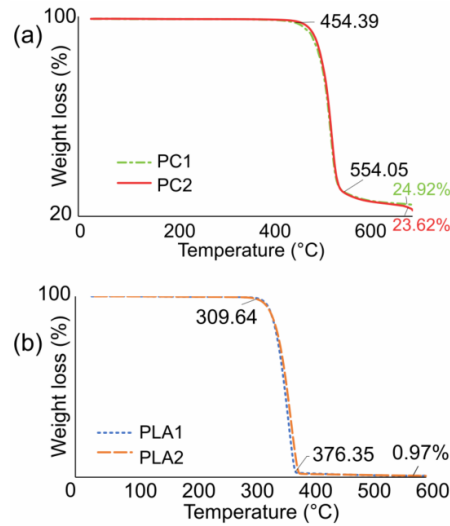


Fig. 5 TGA curves of (a) PCs and (b) PLAs

PLA thermal resistance is much lower than that of PC. The protocols for heat curing of the inks, originally planned for PC substrates, have to be re-evaluated to limit possible thermal damages of PLA (see section 5.2).

We determined the exact mechanical properties of our PC and PLA grades (Table 5) and the data will be useful for the demonstrator in section 5.4. The experimental values correspond to literature ones except for Young's moduli which are lower. As expected, PC1 has good mechanical properties as demonstrated by its elastic modulus (Young) and the remarkably high elongation at break. This is explained in literature by the mechanism of elastic recovery for PC sheets [45]. In other respects, PLA films were tested in two different manners, with stretching in the direction of the film extrusion (//) and perpendicular to the direction of extrusion (\perp). The mechanical properties of PLA are better in the direction of extrusion with an elongation at break of 4% against 2.5% when perpendicular to extrusion. PLA1 has even a higher Young's modulus than PC1 (3000 MPa vs. 2130 MPa) and is thus less prone to warping than PC1. However, these tensile tests proved that PLA is a very brittle polymer compared to PC with an elongation at break of less than 4%, compared to about 130% for PC. This is explained in literature by the mechanism of failure related to the internal stresses in PLA samples [46]. Another comparison is in the tensile strength values. We clearly see that PC1 and PLA1 (//) have similar tensile strength at break in the order of 60 N/mm². Therefore, both materials can support without fracture a similar load when being stretched, demonstrating interesting mechanical characteristics for PLA1 (//).

Table 5 Tensile properties of PC1 and PLA1 films at room temperature

	Experimental			Literature [24, 47-49]		
	Young's Modulus (MPa)	Tensile strength at break (N/mm ²)	Elongation at break (%)	Young's Modulus (MPa)	Tensile strength at break (N/mm ²)	Elongation at break (%)
PC1	2132 ± 59	65 ± 2	128.7 ± 16.7	2350	65	100
PLA1 (\perp)	3006 ± 33	53 ± 1	2.6 ± 0.2	3200	50-60	2-10
PLA1 (//)	2971 ± 73	59 ± 3	3.9 ± 0.2	3200	50-60	2-10

Table 6 summarizes experimental values of the impact resistance of the injection grades of the polymers as a mean value of 5 specimens for each sample. PLA specimens were broken with a 1J pendulum and PC specimens were broken with a 15J pendulum. An observation of the cracking pattern for unnotched PLA2 specimens (impact resistance of about 14 kJ/m²) showed that the specimens are shattered in several pieces in the impact area of the pendulum whereas unnotched PC2 specimens are not broken during the test. So, the 15J pendulum did not have enough potential energy to break unnotched PC specimens. Therefore, notching the PC specimens was necessary to obtain conclusive results. Then, considering that the energy required to break the PLA specimens is much lower than the energy required to break the PC specimens, the impact resistance for notched specimens of PLA2 is very low (about 2 kJ/m² with 1J pendulum) compared to the value for notched PC2 specimens (about 9 kJ/m² with 15J pendulum). Thus, we confirmed that PLA2 is brittle and PC2 quite ductile.

Table 6 Impact resistance of PC2 and PLA2 specimens at room temperature (Charpy test)

Specimen – pendulum	Impact resistance (kJ/m ²)	Literature [50, 51]
PC2 (notched) – 15J	8.9 ± 0.2	6.90 (25J pendulum)
PLA2 (unnotched) – 1J	13.7 ± 0.6	19 ± 5
PLA2 (notched) – 1J	1.7 ± 0.3	2.5 ± 0.6

The surface roughness of the injected polymers (PC2 and PLA2) was not measured because it only depends on the surface roughness of the injection mold. We measured surface roughness of PC1 and PLA1 before screen-printing, because this may have an influence on the printed pattern. Fig. 6 compares the microscopic pictures of PC1 and PLA1 surface films with the surface roughness measurements obtained with RH-2000 Hirox microscope and NPS-NP3 confocal profilometer. Observing the microscopic pictures, PLA1 presents oriented defects whereas PC1 has no visible defects. These defects may be reduced by optimization of the extrusion process. Furthermore, the confocal profilometer shows the smooth finish of the commercial PC1 films and the slight irregularity on the PLA1 surface corresponding to the extrusion process. Both PC and PLA surface roughness Sa are in the same range, with 0.19 μm to 0.45 μm for PC and 0.37 μm to 0.88 μm for PLA.

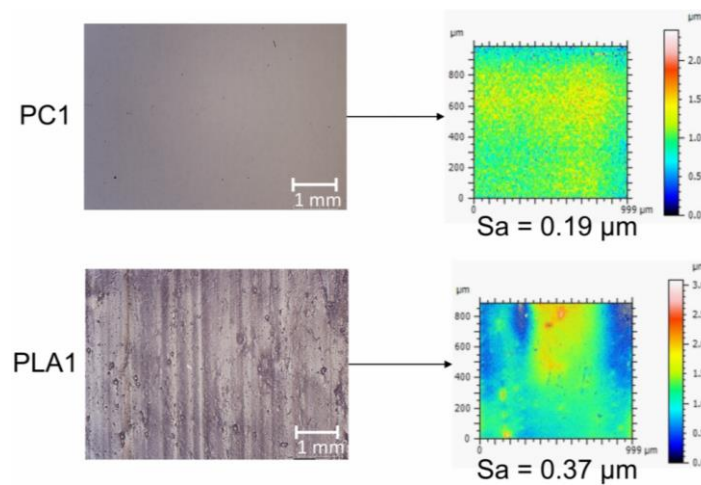
**Fig. 6** Measurements with a confocal profilometer of the surface roughness Sa of PC1 and PLA1 films

Table 7 presents experimental surface properties of the polymer materials as this may have some importance during over-molding. The water contact angles and the surface energy match with the values presented in literature [52, 53]. Contact angle measurements are mainly affected by roughness, interfacial tension and molecular orientation in the polymer material. All PC and PLA have water contact angles in the range of 74-84°, with PLA surfaces more hydrophilic than PC surfaces because of PLA chemical bonds interacting with water. PC1, PC2 and PLA2 have similar surface energies around 46 mN/m. However, PLA1 has a lower surface energy than the ones of the other polymer grades: it can be explained by the previous observation in Fig. 6 with the irregularities, defects of the film surface, slightly increasing its roughness. The roughness also affected the precision of the results and the surface energy of PLA1 presents the largest uncertainty of measurements. Therefore, considering both surface roughness and surface properties, it is expected to get similar results during screen printing (quality of printed patterns before curing and adhesion after curing).

Table 7 Surface properties of the polymer materials

	Water contact angle (°)	Surface energy (mN/m)
PC1	84.8 ± 3.4	45.8 ± 0.9
PC2	78.7 ± 2.1	46.8 ± 2.0
PLA1	79.3 ± 4.5	37.8 ± 6.3
PLA2	73.7 ± 4.1	45.7 ± 2.8

5.2. Screen printing ink and conductive adhesive study

Depending on the application, inks of different nature (conductive, dielectric, decoration) may be used in the IME process by screen printing. IME commercial inks are available from different suppliers (DuPont, Loctite

Henkel, Encre Dubuit, etc.) and have mainly been tested for good adhesion and stretching properties on PC films.

The TGA and DSC analyses for ME603 are shown in Fig. 7. During TGA characterization, the mass of the sample decreases as the temperature increases, steadying at 58% of the initial mass. The solid content of the ink is about 60%, which is in good agreement with the 50-60% silver particles in the manufacturer datasheets. Comparing DSC and TGA, the first step of the mass reduction can be identified as a 34% quick drop of sample mass between 40°C and 250°C. This corresponds to the evaporation of the solvents shown by the endothermic reaction on the DSC curve. After 250°C, residual solvents are decomposed and evaporated. The traces cured at lower temperature (80°C) still have interesting properties for stretchable applications.

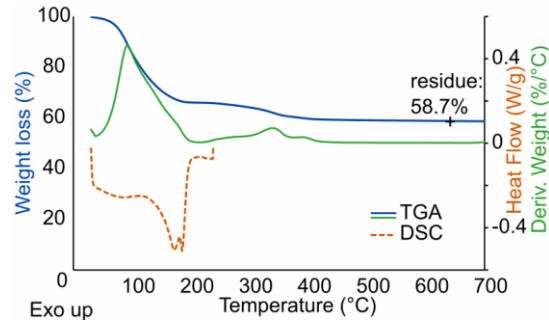


Fig. 7 Weight loss and Derivative Weight loss (lines) during TGA and DSC curve (dash) of ME603 ink

Considering T_g of PLA1 at 54.9°C, it is not wise to cure PLA films at the temperature recommended by the supplier for PC (120°C). But the weight derivative curve for ME603 shows an optimum of solvent evaporation for the ink at 90°C. So, we checked if it is possible to obtain acceptable resistivity of the ink at lower temperature. An isothermal TGA study at 120°C and at 55°C (just at T_g of PLA) was carried out to observe the solvent evaporation behavior in the ME603 ink and to determine the ink heat curing time. The result is presented in Fig. 8 for two isotherms, one hour at 120°C and 36 hours at 55°C. A rule of thumb was to choose curing times to achieve similar weight loss (solvent evaporation) at both temperatures. The supplier recommends drying the ink on PC at 120°C for 20 minutes representing a residue of approximately 73%, which corresponds to a drying time of 142 min (2h22) at 55°C, which is suitable for PLA. Therefore, we decided to apply the following drying conditions for curing ME603 ink on PLA: 55°C for 2h30.

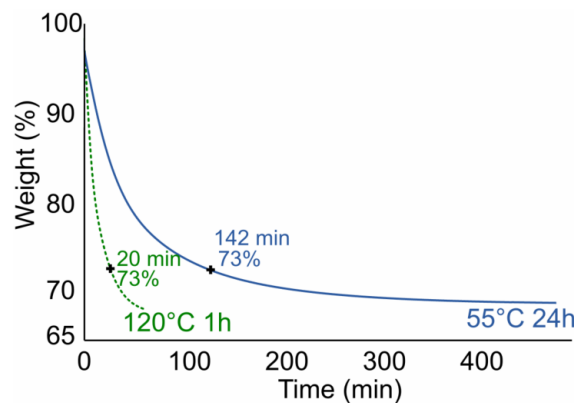


Fig. 8 TGA isothermal study of ME603 ink at 120°C for 1 h (dots) and at 55°C for 24 h (line). A correction time of 15 minutes was applied on both curves to compensate the heating and stabilization stage to the isothermal temperature of the TGA from room temperature.

The printed patterns on PC1 and PLA1 are similar in terms of width and thickness (Fig. 9). The thickness of the screen-printed ink is about 5-9 μm on both polymers as observed with the cross-sectional views.

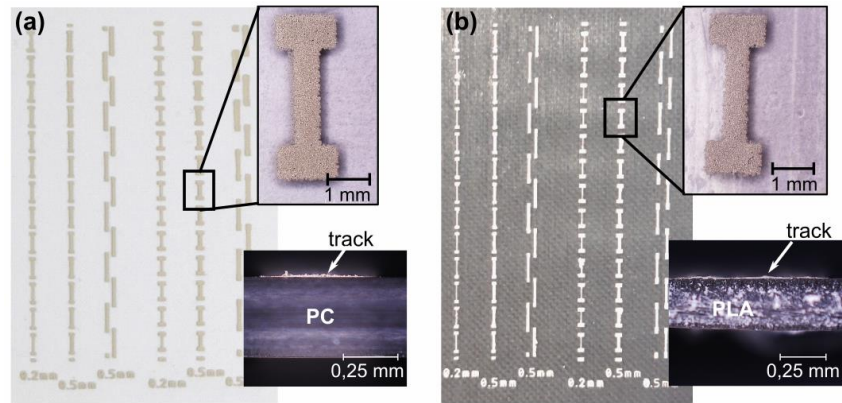


Fig. 9 Observation of the screen-printed patterns of ME603 ink (a) on a PC1 film and (b) on a PLA1 film

The impact of the curing temperature and time on the resistivity of the ME603 ink was quantified and compared to bulk silver and the supplier's data as summarized in Table 8. From the experiments, we can see that the resistivity of ME603 dried at 55°C for 2h30 on PLA1 is about 7 times higher than on PC1 at 120°C for 20 minutes. So, drying the ink at lower temperature induces a significant increase in the resistivity of ME603. Mu et al. [54] shows that if the curing temperature and the curing time increase, the ME603 cured tracks become more conductive but less stretchable. The ME603 ink will thus be less conductive on PLA1 than on PC1, but this is sufficient for an electronic device in IME.

Table 8 Comparison of resistivity values for bulk silver and ME603

	Experimental		Literature	
	ME603 on PC1 (120°C – 20 min)	ME603 on PLA1 (55°C – 2h30)	Bulk silver	ME603 supplier data (120°C – 20 min)
Resistivity ($\mu\Omega\cdot\text{cm}$)	31 – 54	290 – 300	1.59	≤ 90

With a sharp tool, crossed lines were engraved in a grid pattern as shown in Fig. 10. Looking at the classification of test results, we are for both PC and PLA in the category 0, which means that the edges of the cuts are smooth and none of the squares of the lattice are detached. So, we have a great adhesion of ME603 on PC1 and on PLA1 substrates. It is in agreement with the surface properties of the polymers discussed in section 5.1.

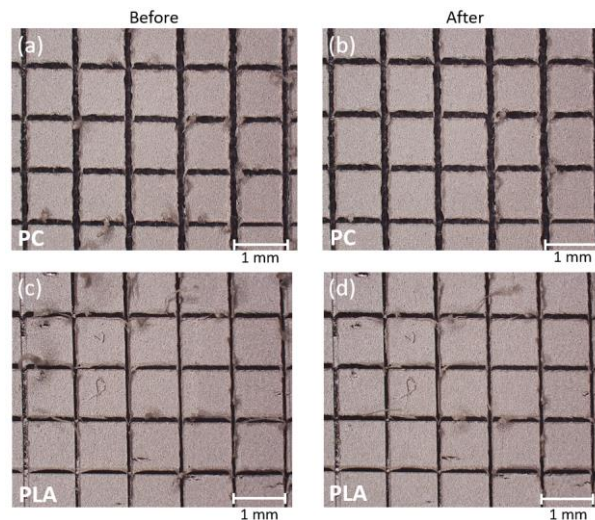


Fig. 10 Standardized scotch test (a-b) on PC1 and (c-d) on PLA1

As explained in Section 1, SMDs are placed on the film and connected to the conductive ME603 pattern with an electrically conductive adhesive, such as ME902 from DuPont (see schematic Fig.1). If necessary non-conductive structural adhesive can also be deposited to secure the SMDs, such as ethyl cyanoacrylate Loctite Superglue-3. Contrary to ME603, these adhesives are not screen printed but dispensed point by point with a manual-semi-automatic dispenser. Another point is that ME902 requires thermal curing whereas the ethyl

cyanoacrylate adhesive cures at room temperature in a few seconds. From the safety datasheets of ME603 and ME902, we can figure out that both compounds have the same chemical nature, hence notably the same major solvent (2-methoxymethylethoxy)propanol. Fig. 11 presents TGA and DSC analyses of the ME902 paste. The mass of the sample decreases as the temperature increases, steadying at 61% of the initial mass. The solid content of the adhesive is therefore in good agreement with the 60-70% silver particles in the manufacturer datasheets. The first step of this decrease is a 25% drop of sample mass between 40°C and 250°C corresponding to the evaporation of the solvents shown by the endothermic reaction on the DSC curve (dash). Residual solvents are decomposed and evaporated after 250°C.

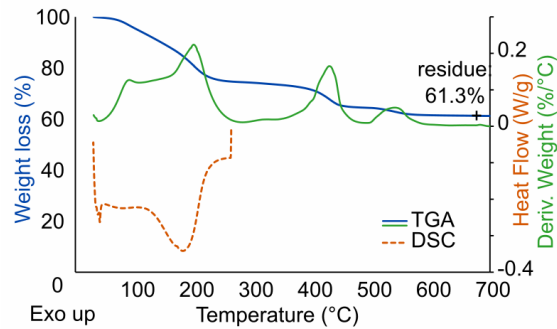


Fig. 11 Weight loss and Derivative Weight loss (lines) during TGA and DSC curve (dash) of ME902 adhesive

So, the ME902 paste has a similar thermal behavior as the ME603 ink. Considering the manufacturer advice to dry both the ink and the adhesive at the same time and temperature on a PC substrate, we applied the same reasoning on PLA substrates. The heat curing time and temperature of the adhesives are set at 55°C for 2h30 on PLA. Furthermore, the choice of an ethyl cyanoacrylate paste (Loctite Superglue-3) as structural adhesive is justified thanks to a room temperature drying capability that won't affect PLA properties.

The 2D test vehicle in Fig. 12a was designed to evaluate the adhesion of standard 0805 and 0603 SMDs. Shear testing is a method that enables to diagnose adhesion problems quickly and effectively. The effect of shearing on the paste joint integrity is the main parameter observed, it gives us information on the fracture surface of the adhesives. On the test vehicle, the ME603 tracks are either 0.5-mm or 0.2-mm wide and 0.4-mm or 0.6-mm long. The SMDs are placed in a longitudinal or transversal manner but it does not impact the adhesion strength because the shear test is done using a rotary tool tip enabling to perfectly align the tool tip with the component.

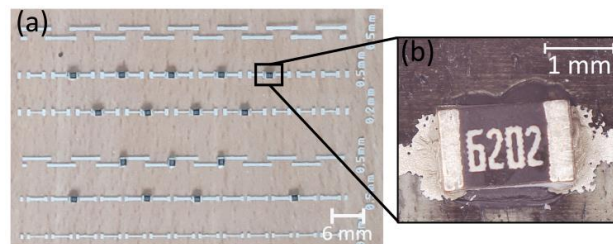


Fig. 12 (a) ME603 test vehicle on PLA1, (b) SMD connected with ME902 adhesive and Loctite Superglue-3

Shearing tests were carried out to determine the adhesion strength of ME902 alone on the ME603 tracks. This gives us a reference value for the adhesion strength of the conductive adhesive on PC1 and PLA1. Table 9 summarizes the results of the shear testing as a mean value on 10 specimens for each set of conditions to determine the impact of the fracture surface on the adhesion strength of the SMD. First, we compared the drying conditions of ME902 on PC1. The shear stress is close to three times higher when ME902 is dried at 120°C for 20 minutes (7.68 N/mm²) than when it is dried at 55°C for 2h30 (2.76 N/mm²). So, when the drying temperature decreases, so does the adhesion strength. At 55°C, the adhesion is weaker because the paste is not optimally dried: some organic solvent remains as we can see with the TGA curve in Fig. 11, where the optimal temperature of solvent evaporation (wide peak between 90°C and 190°C) for ME902 is not reached. Then, for the same drying conditions (55°C – 2h30), the shear stress is 1.5 times higher on the PC substrate than on the PLA substrate. So, the adhesion of ME902 on PLA1 is slightly worse than on PC1 at 55°C. This is explained by the difference in fracture surface with the ME603 tracks being slightly removed with the ME902 adhesive on PLA during shearing

and corresponding to the lower surface energy for PLA1 discussed in section 5.1. Finally, considering the adhesion strength of ME902 alone is not optimal at 55°C and to try and reach the reference shear stress we have with PC1 on PLA1, the SMDs were connected with ME902 and secured with Loctite Superglue-3 on ME603 tracks (see Fig.12b). In this case, the shear stress is excellent at about 9 N/mm², it is even higher than the reference on PC1 (7.68 N/mm²) for the optimal drying conditions. This excellent adhesion strength is logical considering that the optimal drying temperature of the structural paste is room temperature. We compared that value for the same conditions of drying temperature and time on PC1 and we concluded that the increase in adhesion strength comes only from the ethyl cyanoacrylate paste, with results in the order of 9 N/mm² for PC1 and PLA1.

Table 9 Shearing test data on PC1 and PLA1 substrates

	Drying conditions	Shear stress (N/mm ²)
ME902 on PC1 (reference)	120°C – 20 min	7.68 ± 0.71
ME902 on PC1	55°C – 2h30	2.76 ± 0.63
ME902 on PLA1	55°C – 2h30	1.80 ± 0.30
ME902 + Loctite Superglue-3 on PC1	55°C – 2h30	8.67 ± 1.93
ME902 + Loctite Superglue-3 on PLA1	55°C – 2h30	9.10 ± 2.74

Looking at the imprint left by the SMD after shearing on the PLA1 substrate, the fracture surface is placed in the ethyl cyanoacrylate adhesive layer and in the ME902 layer. We can see the structural paste imprint on the PLA substrate (Fig.13a, area in white in the center) and the ME902 paste left on the back of the SMD (Fig.13b). This explains the great increase in shear stress and therefore adhesion strength of the SMD on PLA. Loctite superglue-3 has proven to be an appropriate choice for PLA.

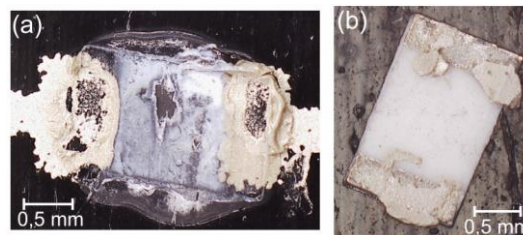


Fig. 13 Torn SMD on PLA1 for ME902 + Loctite Superglue-3 dried at 55°C for 2h30, (a) imprint left by SMD and (b) back of SMD, pictures taken with a numerical microscope

5.3. Thermoforming and injection molding of PLA electronic films

We used cone-shaped and cylinder-shaped molds like Gong et al. [32] to study the effect of the geometrical parameters (fillet radius and draft angle) on the film deformation. Positive vacuum forming was carried out. Using the T-SIM software, we did a preliminary study in simulation of the thermoforming process. The detailed parameters for T-SIM are listed in SI2. The simulation focuses on the variation of film thickness: the comparison between simulation and experimental work is presented in details for PC in SI3. The main conclusion is that the same tendencies are observable in simulation and in the experimental work: the thickest areas and the thinnest areas are at the same place along the cross section. Therefore, the experiment and the simulation are in accordance.

For PLA, the film is thermoformed at 110°C. Considering the initial thickness of PLA1 films is smaller than PC1 films (300 μm vs. 375 μm) and PLA is not in the material database of T-SIM, it is not possible to compare their cross section as such. We can however perform a qualitative study of the thermoforming of PLA1 and compare it to PC1. Using a screen-printed pattern of ME603 dried at 120°C for 20 min on PC1 and at 55°C for 2h30 on PLA1, we observed the deformation of the grid lines Fig. 14 that shows where the stretching of the film is more important. This qualitative study proves firstly that PLA1 300-μm-thick films are thermoformable without any cracks or holes appearing in the film or the ME603 ink and secondly, the grid pattern is qualitatively deformed in the same way on PC1 and PLA1. Therefore, the areas of greater deformations are the same for PC1 and PLA1 which confirms that the thickness of PLA1 films will vary in the same manner as PC1 films.

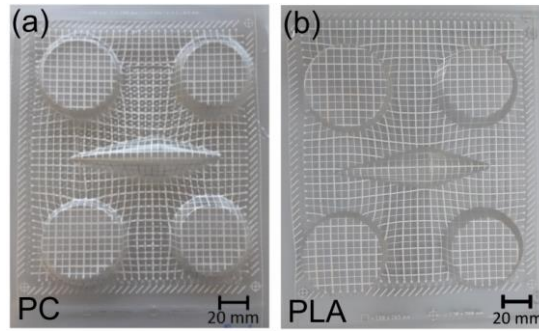


Fig. 14 Thermoformed ME603 grid pattern (a) on PC1 film and (b) on PLA1 film

Finally, a more detailed observation of the ME603 ink on PLA1 films was carried out. A cone-shaped mold of thickness 1.5 mm was used to thermoform a ME603 pattern with SMD components as presented Fig. 15. No cracks in the ink or tear of the SMDs are observed after thermoforming and thus the quality of PLA thermoformed electronic films is good.

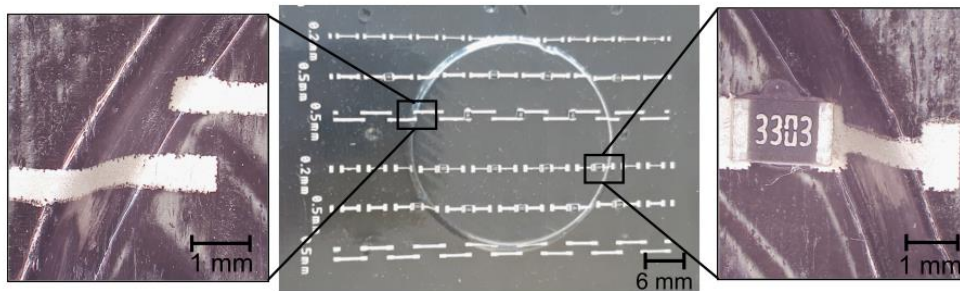


Fig. 15 Thermoformed PLA1 film with ME603 tracks and SMDs

Last, we determined the feasibility of PLA injection in the IME process. Using the test vehicle presented in section 5.2 and the two injection molds described in section 3.5, the following optimized injection parameters were obtained for PLA: temperature of polymer melt at 200°C, injection mold at room temperature and screw speed at 60 mm/s. For PC, the temperature of polymer melt is increased at 300-310°C and the Injection Mold 1 is at 110°C. On one hand, outside the areas with conductive patterns or SMDs, the injection of PLA2 on PLA1, and PC2 on PC1, ran smoothly. The adhesion of the injected plate on the polymer film was qualitatively excellent because the two polymers are of the same chemical nature. In other words, the adhesion PLA2/PLA1, and PC2/PC1, is excellent. On the other hand, the SMDs were glued and dried at 55°C for 2h30 for PLA1, and following the same conditions with an additional 120°C for 6 minutes for PC1. As a first step, only the conductive adhesive ME902 was used to glue the SMDs. A slight wash out of the electronic components was observed during the injection of PLA2 and PC2 when using the mold with the side injection point. It is less visible for PLA than for PC because the higher temperature of polymer melts during the injection of PC causes the SMDs to be pushed further. The microscopic pictures in SI4 show this SMD displacement in the direction of the injection flow. This mainly demonstrates the importance of using a structural adhesive to reinforce the adhesion strength on the polymer film. So, as a second step, the SMDs were glued with ME902 and ethyl cyanoacrylate. As shown in Fig. 16, the injection of PLA2 on the PLA1 electronic film has no effect on the position of the ink and the electronic components: they have not moved or been washed out. The device in section 5.4 will demonstrate the functionality of the electronic circuit after injection.

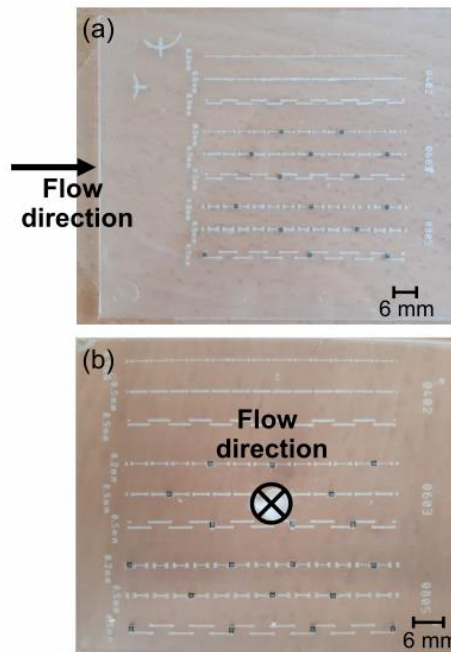


Fig. 16 Injection molding of PLA2 on a screen-printed PLA1 film. The conductive ink is ME603 and the SMDs are glued with ME902 and ethyl cyanoacrylate. (a) Injection Mold 1, (b) Injection Mold 2

The wash out of the SMDs is only observed when the ME902 paste is used alone and for a side injection point. Therefore, for an optimal device in the next section, the use of the structural adhesive and the mold with the central injection point (Injection Mold 2) are favored.

5.4. Functional device

The manufacturing of a simple IME device on PLA is reported below to demonstrate the proof of concept (PLA and IME). The electronic circuit is based on a NE555 IC timer [55] with three resistances, one capacitor and one LED. All electronic components are SMDs and the thickest component is the NE555 IC with a height of 1.8 mm. Metallic rivets are incorporated to connect the device to an external power supply. For the sake of simplicity, thermoforming and over-molding are performed separately and we tested if the circuit is operational at each step of the IME process. The device after screen printing of the conductive tracks and connected SMDs and rivets is shown in Fig. 17a. PLA1 electronic film was thermoformed at 110°C by vacuum forming against a cylindrical tool (1.5 mm high, 40 mm in diameter, 30° draft angle) as presented in Fig. 17b, and then over-molded with PLA2 using Injection Mold 2 as observed in Fig. 17c. The result is a functional device with an overall thickness of PLA of about 3.2 mm.

Although it is shown that PLA is brittle as reported in section 5.1, it should be noted that we have in our hands a part with interesting structural rigidity and surprising resistance to shocks (the part does not break when it falls on the ground). This result is very promising. Additionally, PLA has proven to be sufficiently translucent for lighting and waveguiding applications, so applications can be considered for HMIs.

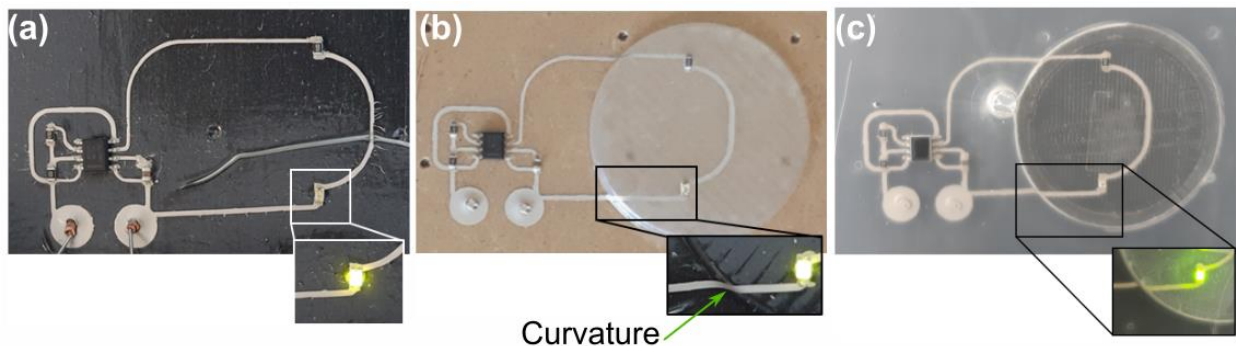


Fig. 17 Electronic circuit (a) after curing, (b) after thermoforming, (c) after injection molding

6. Discussion

In this paper, we demonstrated the feasibility of In Mold Electronics on Poly(Lactic Acid). Even if PC has an excellent thermal stability up to 140°C and a great impact resistance which makes it a suitable candidate for IME, PLA has also several interesting characteristics: it is biosourced and biodegradable (few polymers are both), it has a very high rigidity and a great chemical reactivity which is an advantage for the adhesion of the screen-printing inks and pastes. Even though the low T_g of PLA was a disadvantage, we managed to heat cure the conductive ink and paste by lowering the temperature and increasing the drying time. However, we lost in ink conductivity (resistivity of about 40 μΩ.cm on PC and 295 μΩ.cm on PLA) although it was good enough to demonstrate the proof of concept. A potential solution may be the use of photonic curing to dry the ink faster and at a much higher temperature without impacting the polymer substrate [56]. Photonic soldering may also be considered to replace conductive and non-conductive pastes with brazing pastes.

In other respects, the brittleness of PLA seemed in a first approach unfavorable for IME. But we noticed that our demonstrator features interesting mechanical strength and surprising resistance to shock when dropped on the floor. Moreover, it should be possible to develop a PLA with improved resistance to shock and elongation at break. Indeed, numerous papers tackle the issue of improving the mechanical and/or thermal properties of PLA [30, 57]. Several methods exist (copolymerization, use of impact modifiers, fillers, etc) but it has been shown that when a property is improved, another one is usually changed in a negative way. The mechanical properties of PLA are modified with an increase in crystallinity, such as a higher Young's modulus and toughness which means an increase in brittleness. However, a trade-off is required and super engineered PLA are starting to appear with excellent thermal or mechanical properties [58].

During thermoforming and over-molding, PLA requires much lower temperatures than PC, giving it a significant advantage for industrial scale applications with a lower environmental impact. Furthermore, the tendency of the PLA sheets to fall down quickly when heated, makes it a very easy material to deform and shape in thermoforming. Also, the lower temperature of the PLA melt in injection leads to lesser wash out issue than with PC. A point that remains to be analyzed is the aging of IME devices made with PLA (under specific temperature, humidity, etc) especially because PLA is less resistant to heat than PC.

Finally, among many possibilities, PLA can be easily degraded either by industrial composting (58°C, 6 months for 90% degradation), by thermophilic anaerobic digestion (52°C) [59] or chemically degraded [60]. It can also be mechanically recycled and even depolymerized by hydrolysis [61], by alcoholysis or using enzymes [62, 63].

7. Conclusion

The use of PLA at every step of the In Mold Electronics process was achieved. In this study, PLA films of suitable thickness for IME (about 300 μm) were manufactured by extrusion and used as substrates. The ink used for printing the conductive pattern has good adhesion with PLA substrates according to ISO 2409 standard, even if it has been cured at a temperature below the supplier's specifications. The ink resistivity on PLA is about 295 μΩ.cm for the ME603 silver ink cured for 2h30 at 55°C and is sufficient for an electronic circuit to work. The adhesion of the SMDs connected to the circuit with ME902 conductive paste and Superglue-3 structural adhesive was also characterized with a suitable shear strength of 9 N/mm². During thermoforming, the thermomechanical behavior of PLA made it easy to give a 3D shape to the circuit. Finally, during over-molding with PLA, ink, adhesives and electronic components were not washed out. This was facilitated by the melt temperature of 210°C during the injection. The final object has interesting mechanical resistance and optical properties.

The IME on PLA has great potential and the process is open to improvement towards mass production on an industrial scale. Developing complex 3D injection molds enables to study larger deformations of PLA films during thermoforming as well as over-molding in more realistic conditions. Another pragmatic solution consists in blending PC and PLA, especially for improved thermal properties. It has been industrially done for injected parts only (mobile phones for example). However due to the difference in chemical nature between PC and PLA, one of the main problems would be the dismantling and recycling of the PC/PLA blend. Therefore, the choice of an all PLA device is justified.

In the long term, PLA could eventually replace petroleum-based polymers like PC as a greener, bio-based and biodegradable alternative in many applications. The idea is to extend the lifespan of devices but they could suffer from the poor thermal performances of PLA, hence the necessity to study the aging of IME devices made with PLA. Recyclability is a considerable advantage and could open the way to a circular economy of IME, at a time when the dismantling of conventional IME devices is a major problem.

Acknowledgments

This work has been financially supported by the Auvergne-Rhône-Alpes Region, Pack Ambition Recherche 2020, Convention n°[20 009551 01 - 22464](#), BioAntenna project (Antenne pour IoT sur polymère biodégradable pour le stockage et la récupération d'énergie) that we gratefully acknowledge.

Declarations

Funding This work has been financially supported by the Auvergne-Rhône-Alpes region.

Competing interest The authors declare no competing interest.

Data availability Data and materials are presented in the manuscript and in the supplementary information.

Code availability Not applicable.

Ethics approval and consent to participate Not applicable.

Consent for publication All authors have agreed to the submitted version of the manuscript.

References

- [1] N. Heininger, M. Kivikoski, Y.-H. Lee (2005) Advanced antennas for mobile phones. *Proceedings of International Symposium on Antennas*
- [2] J. Y. Chen, W. B. Young (2013) Two-Component Injection Molding of Molded Interconnect Devices. *Advanced Materials Research* 628:78–82. <https://doi.org/10.4028/www.scientific.net/AMR.628.78>
- [3] D. Unnikrishnan (2015) Mid technology potential for RF passive components and antennas. Dissertation, Université de Grenoble, France
- [4] C. Goth, S. Putzo, J. Franke (2011) Aerosol jet printing on rapid prototyping materials for fine pitch electronic applications. *IEEE 61st Electronic Components and Technology Conference (ECTC)*. <https://doi.org/10.1109/ECTC.2011.5898664>
- [5] S. M. Bidoki, D. M. Lewis, M. Clark, A. Vakorov, P. A. Millner, D. McGorman (2007) Ink-jet fabrication of electronic components. *J. Micromech. Microeng.* 17:967–974. <https://doi.org/10.1088/0960-1317/17/5/017>
- [6] J. Franke (2014) Three-dimensional molded interconnect devices (3D-MID). Carl Hanser Verlag, München
- [7] TactoTek, "This is IMSE". <https://www.tactotek.com/this-is-imse/>. Accessed May 18, 2022
- [8] J. Vanfleteren, F. Bossuyt, B. Plovie (2016) A new technology for rigid 3D free-form electronics based on the thermoplastic deformation of flat standard PCB type circuits. *12th International Congress Molded Interconnect Devices (MID)*. <https://doi.org/10.1109/ICMID.2016.7738924>
- [9] C. Kallmayer, F. Schaller, T. Löher, J. Haberland, F. Kayatz, A. Schult (2018) Optimized Thermoforming Process for Conformable Electronics. *13th International Congress Molded Interconnect Devices (MID)*. <https://doi.org/10.1109/ICMID.2018.8526929>
- [10] T. Gerges, A. Marie, T. Wickramasinghe et al (2021) Investigation of 3D printed polymer-based heat dissipator for GaN transistors. *23rd European Conference on Power Electronics and Applications (EPE'21 ECCE Europe)*. hal-03451785
- [11] DuPont de Nemours & Co (2019) Functional Ink Systems for "In Mold Electronics". <https://www.dupont.com/products/in-mold-electronic-technology.html>. Accessed 10 January 2022
- [12] R.-H. Kim, D.-H. Kim, J. Xiao et al (2010) Waterproof AlInGaP optoelectronics on stretchable substrates with applications in biomedicine and robotics. *Nature Materials*. <https://doi.org/10.1038/nmat2879>
- [13] M. Bakr, F. Bossuyt, J. Vanfleteren, Y. Su (2020) Flexible microsystems using over-molding technology. *Procedia Manufacturing* 52:26–31. <https://doi.org/10.1016/j.promfg.2020.11.006>
- [14] T. Simula, P. Niskala, M. Heikkinen, O. Rusanen (2018) Component Packages for IMSE (Injection Molded Structural Electronics). *IMAPS Nordic Conference on Microelectronics Packaging (NordPac)*. <https://doi.org/10.23919/NORDPAC.2018.8423845>
- [15] A. Wimmer, H. Reichel, B. Rauch, R. Schramm, J. Hörber, B. Hässler (2016) Manufacturing of sandwich structures for the integration of electronics in in mold labelling components. *12th International Congress Molded Interconnect Devices (MID)*. <https://doi.org/10.1109/ICMID.2016.7738922>
- [16] DuPont de Nemours & Co (2014) Thermoformable polymer thick film silver conductor and its use in capacitive switch circuits. Patent US8692131 B2
- [17] NaturePlast (2017) Bioplastiques : évolution du marché 2017-2022. <https://natureplast.eu/es/marche-des-bioplastiques-20172022/>. Accessed 18 May 2022

- [18] NaturePlast (2021) Les bioplastiques en 2020. <http://natureplast.eu/bioplastiques-en-2020-legislation-france/>. Accessed May 18, 2022
- [19] J. Payne, M. D. Jones (2021) The Chemical Recycling of Polyesters for a Circular Plastics Economy: Challenges and Emerging Opportunities. *ChemSusChem* 14:4041–4070. <https://doi.org/10.1002/cssc.202100400>
- [20] H. Schnell (1959) Linear Aromatic Polyesters of Carbonic Acid. *Ind. Eng. Chem.* 51:157–160. <https://doi.org/10.1021/ie50590a038>
- [21] R. Auras, B. Harte, S. Selke (2004) An Overview of Polylactides as Packaging Materials. *Macromol. Biosci.* 4:835–864. <https://doi.org/10.1002/mabi.200400043>
- [22] M. K. Välimäki, L. I. Sokka, H. B. Peltola et al (2020) Printed and hybrid integrated electronics using bio-based and recycled materials—increasing sustainability with greener materials and technologies. *Int J Adv Manuf Technol* 111:325–339. <https://doi.org/10.1007/s00170-020-06029-8>
- [23] E. Balla, V. Daniilidis, G. Katlioti et al (2021) Poly(lactic Acid): A Versatile Biobased Polymer for the Future with Multifunctional Properties—From Monomer Synthesis, Polymerization Techniques and Molecular Weight Increase to PLA Applications. *Polymers* 13:1822. <https://doi.org/10.3390/polym13111822>
- [24] E. Luoma, M. Välimäki, T. Rokkonen et al (2021) Oriented and annealed poly(lactic acid) films and their performance in flexible printed and hybrid electronics. *Journal of Plastic Film & Sheeting* 0:1–34. <https://doi.org/10.1177/8756087920988569>
- [25] S. Inkinen, M. Hakkarainen, A.-C. Albertsson, A. Södergård (2011) From Lactic Acid to Poly(lactic acid) (PLA): Characterization and Analysis of PLA and Its Precursors. *Biomacromolecules* 12:523–532. <https://doi.org/10.1021/bm101302t>
- [26] J.-R. Sarasua, R. E. Prud'homme, M. Wisniewski, A. Le Borgne, N. Spassky (1998) Crystallization and Melting Behavior of Polylactides. *Macromolecules* 31:3895–3905. <https://doi.org/10.1021/ma971545p>
- [27] D. Garlotta (2001) A Literature Review of Poly(Lactic Acid). *Journal of Polymers and the Environment* 9:63–84. <https://doi.org/10.1023/A:1020200822435>
- [28] M. Jamshidian, E. A. Tehrani, M. Imran, M. Jacquot, S. Desobry (2010) Poly-Lactic Acid: Production, Applications, Nanocomposites, and Release Studies. *Comprehensive Reviews in Food Science and Food Safety* 9:552–571. <https://doi.org/10.1111/j.1541-4337.2010.00126.x>
- [29] N. J. Teh, P. P. Conway, P. J. Palmer, S. Prosser, A. Kioul (2000) Statistical optimisation of thermoplastic injection moulding process for the encapsulation of electronic subassembly. *Journal of Electronics Manufacturing* 10:171–179. <https://doi.org/10.1142/S0960313100000150>
- [30] V. Nagarajan, A. K. Mohanty, M. Misra (2016) Perspective on Polylactic Acid (PLA) based Sustainable Materials for Durable Applications: Focus on Toughness and Heat Resistance. *ACS Sustainable Chem. Eng.* 4:2899–2916. <https://doi.org/10.1021/acssuschemeng.6b00321>
- [31] D. G. Legrand, J. T. Bendler (1999) *Handbook of Polycarbonate Science and Technology*. CRC Press
- [32] Y. Gong, K. J. Cha, J. M. Park (2020) Deformation characteristics and resistance distribution in thermoforming of printed electrical circuits for in-mold electronics application. *Int J Adv Manuf Technol* 108:749–758. <https://doi.org/10.1007/s00170-020-05377-9>
- [33] G. A. Adam, J. N. Hay, I. W. Parsons, R. N. Haward (1976) Effect of molecular weight on the thermal properties of polycarbonates. *Polymer* 17:51–57. [https://doi.org/10.1016/0032-3861\(76\)90153-1](https://doi.org/10.1016/0032-3861(76)90153-1)
- [34] J. Wiklund, A. Karakoç, T. Palko et al (2021) A Review on Printed Electronics: Fabrication Methods, Inks, Substrates, Applications and Environmental Impacts. *J. Manuf. Mater. Process.* 5:89. <https://doi.org/10.3390/jmmp5030089>
- [35] M. Hatala, P. Gemeiner, M. Hvojník, M. Mikula (2018) The effect of the ink composition on the performance of carbon-based conductive screen printing inks. *J Mater Sci: Mater Electron* 30:1034–1044. <https://doi.org/10.1007/s10854-018-0372-7>
- [36] S. Merilampi, T. Laine-Ma, P. Ruuskanen (2009) The characterization of electrically conductive silver ink patterns on flexible substrates. *Microelectronics Reliability* 49:782–790. <https://doi.org/10.1016/j.microrel.2009.04.004>
- [37] G. Gruenwald (2018) *Thermoforming: A Plastics Processing Guide, Second Edition*. Routledge
- [38] H. Wei (2021) Optimisation on Thermoforming of Biodegradable Poly (Lactic Acid) (PLA) by Numerical Modelling. *Polymers* 13:654. <https://doi.org/10.3390/polym13040654>
- [39] S.-J. Liu, C.-M. Hsu, P.-W. Chang (2012) Parameters Affecting the Ink Wash-off in In-mold Decoration of Injection Molded Parts. *International Polymer Processing* 27:224–230. <https://doi.org/10.3139/217.2506>
- [40] DuPont de Nemours. Accueil | DuPont France. <https://www.dupontdenemours.fr/>. Accessed 15 June 2022
- [41] L. Delbreilh, A. Bernès, C. Lacabanne, J. Grenet, J.-M. Saiter (2005) Fragility of a thermoplastic polymer. Influence of main chain rigidity in polycarbonate. *Materials Letters* 59:2881–2885. <https://doi.org/10.1016/j.matlet.2005.04.034>
- [42] J. Zhang, Y. Duan, H. Sato et al (2005) Crystal Modifications and Thermal Behavior of Poly(L-lactic acid) Revealed by Infrared Spectroscopy. *Macromolecules* 38:8012–8021. <https://doi.org/10.1021/ma051232r>
- [43] L.-T. Lim, R. Auras, M. Rubino (2008) Processing technologies for poly(lactic acid). *Progress in Polymer Science* 33:820–852. <https://doi.org/10.1016/j.progpolymsci.2008.05.004>
- [44] H. Houichi, A. Maazouz, B. Elleuch (2015) Crystallization behavior and spherulitic morphology of poly(lactic acid) films induced by casting process. *Polym Eng Sci* 55:1881–1888. <https://doi.org/10.1002/pen.24028>
- [45] A. Rosa-Sainz, G. Centeno, M. B. Silva, J. A. López-Fernández, A. J. Martínez-Donaire, C. Vallengano (2020) On the Determination of Forming Limits in Polycarbonate Sheets. *Materials* 13:928. <https://doi.org/10.3390/ma13040928>

- [46] L. Cui, B. Imre, D. Tátraaljai, B. Pukánszky (2020) Physical ageing of Poly(Lactic acid): Factors and consequences for practice. *Polymer* 186:122014. <https://doi.org/10.1016/j.polymer.2019.122014>
- [47] C. Penu, M. Helou (2017) Acide polylactique (PLA). *Techniques de l'Ingénieur*. AM3317 V1
- [48] K. Issaadi (2015) Étude des propriétés thermiques et de la morphologie des nanobiopolymères à base de poly acide lactique: effet de la composition et de la nature de la nanocharge. Dissertation, Université A.Mira-Béjaia, Algeria
- [49] J.-M. Dumont (2007) Polycarbonates. *Techniques de l'Ingénieur*. AM3381 V1
- [50] T. Krausz, I. Ailinei, S. V. Galatanu, L. Marsavina (2021) Charpy impact properties and numerical modeling of polycarbonate composites. *Mat Design & Process Comm* 3:e260. <https://doi.org/10.1002/mdp2.260>
- [51] R. Jaratrotkamjorn, C. Khaokong, V. Tanrattanakul (2012) Toughness enhancement of poly(lactic acid) by melt blending with natural rubber. *J. Appl. Polym. Sci.* 124:5027-5036. <https://doi.org/10.1002/app.35617>
- [52] I. Saarikoski, M. Suvanto, T. A. Pakkanen, (2009) Modification of polycarbonate surface properties by nano-, micro-, and hierarchical micro-nanostructuring. *Applied Surface Science*. 255:9000-9005. <https://doi.org/10.1016/j.apsusc.2009.06.073>
- [53] J. R. Rocca-Smith, T. Karbowski, E. Marcuzzo et al (2016) Impact of corona treatment on PLA film properties. *Polymer Degradation and Stability*. 132:109-116. <https://doi.org/10.1016/j.polymdegradstab.2016.03.020>
- [54] Q. Mu, C. K. Dunn, L. Wang, M. L. Dunn, H. J. Qi, T. Wang (2017) Thermal cure effects on electromechanical properties of conductive wires by direct ink write for 4D printing and soft machines. *Smart Mater. Struct.* 26:045008. <https://doi.org/10.1088/1361-665X/aa5cca>
- [55] Texas Instruments (1973) NE555 IC Timer specifications. <https://www.ti.com/lit/ds/symlink/ne555.pdf>. Accessed 25 May 2022
- [56] A. V. Quintero, N. Frolet, D. Märki et al (2014) Printing and encapsulation of electrical conductors on polylactic acid (PLA) for sensing applications. *IEEE 27th International Conference on Micro Electro Mechanical Systems (MEMS)*. <https://doi.org/10.1109/MEMSYS.2014.6765695>
- [57] D. Notta-Cuvier, J. Odent, R. Delille et al (2014) Tailoring polylactide (PLA) properties for automotive applications: Effect of addition of designed additives on main mechanical properties. *Polymer Testing* 36:1-9. <https://doi.org/10.1016/j.polymertesting.2014.03.007>
- [58] M. A. Abdelwahab, S. Jacob, M. Misra, A. K. Mohanty (2021) Super-tough sustainable biobased composites from polylactide bioplastic and lignin for bio-elastomer application. *Polymer* 212:123153. <https://doi.org/10.1016/j.polymer.2020.123153>
- [59] M. Carus (2021) Biodegradable Polymers in Various Environments - According to Established Standards & Certification Schemes. <https://renewable-carbon.eu/publications/product/biodegradable-polymers-in-various-environments-according-to-established-standards-and-certification-schemes-graphic-pdf/>. Accessed 11 January 2022
- [60] L. A. Román-Ramírez, P. McKeown, C. Shah, J. Abraham, M. D. Jones, J. Wood (2020) Chemical Degradation of End-of-Life Poly(lactic acid) into Methyl Lactate by a Zn(II) Complex. *Ind. Eng. Chem. Res.* 59:11149-11156. <https://doi.org/10.1021/acs.iecr.0c01122>
- [61] P. Coszach, J.-C. Bogaert, J. Willocq (2010) Recyclage chimique du pla par hydrolyse. Patent WO2010118954A1. <https://patents.google.com/patent/WO2010118954A1/en-20US4325121.pdf>. Accessed 11 January 2022
- [62] M. Hajjghasemi, B. P. Nocek, A. Tchigvintsev et al (2016) Biochemical and Structural Insights into Enzymatic Depolymerization of Polylactic Acid and Other Polyesters by Microbial Carboxylesterases. *Biomacromolecules* 17:2027-2039. <https://doi.org/10.1021/acs.biomac.6b00223>
- [63] Carbios. Enzymatic recycling. <https://www.carbios.com/en/enzymatic-recycling/>. Accessed 18 May 2022